Manifestation of the Adsorbed CO Diffusion Anisotropy Caused by the Structure Properties of the Pd(110) – (1×2) Surface on the Oscillatory Behavior during CO Oxidation Reaction – Monte-Carlo Model

A. V. MATVEEV, E. I. LATKIN, V. I. ELOKHIN and V. V. GORODETSKII

G. K. Boreskov Institute of Catalysis, Siberian Branch of the Russian Academy of Sciences, Pr. Akademika Lavrentyeva 5, Novosibirsk 630090 (Russia)

E-mail: elokhin@catalysis.nsk.su

Abstract

The modelling of self-oscillations and surface autowaves in CO oxidation reaction over Pd(110) has been carried out by means of the Monte-Carlo technique. The synchronous oscillations of the reaction rate and surface coverages are exhibited within the range of the suggested model parameters (under the conditions very close to the experimental observations). The dependencies of the simulation results on the lattice size and on the diffusion intensity have been studied. It has been established that the adsorbed CO diffusion anisotropy does not influence the oscillation kinetics but leads to the appearance of the propagating reaction fronts on the palladium surface elliptically stretched along the [1$\bar{1}$0] direction in close agreement with the known experimental data.

INTRODUCTION

Experimental study of CO oxidation over Pd(110), Pd(210) single crystals [1, 2] has evidently shown that the modification of the catalytic properties of the palladium surface occurs under the particular reaction conditions caused by the penetration of the adsorbed oxygen atoms into the subsurface layer. These modifications could manifest in the reaction kinetics as the critical effects – hysterese, self-oscillations and chemical waves on the surface. It was established [1, 2], that CO + O_2 reaction over palladium can demonstrate the oscillatory dynamics (in the quite narrow pressure and temperature range) at $P(O_2) = 10^{-3}$–10^{-2} Torr and at the ratio $P(O_2)/P(CO) = 100$–1000. The oscillation mechanism is usually assumed to be connected with the change of the oxygen sticking coefficient caused by the reversible subsurface oxygen formation: $O_{ads} \Leftrightarrow O_{ss}$.

Based on the "oxide model" proposed for the explanation of the critical phenomena in CO oxidation reaction over platinum metals [3] different catalytic systems has been modelled using the so-called "traditional approach" (the analysis and solving of differential equation systems corresponding to the detailed reaction mechanism). For example, using the above-mentioned approach the reaction rate and concentration oscillations in CO oxidation reaction over Pd(110) [4] and Pt(110) [5] has been simulated. However, due to the use of modern physical methods for studying catalytic surfaces, the adsorbate distribution even on the single-crystal surfaces has been found to be substantially non-uniform, and a wide spectrum of spatio-temporal structures (solitons, spiral and travelling waves, chaotic alternating of islands of different adsorbates resembling the turbulent motions, *etc.*) is observed on the surface in the course of numerous catalytic reactions. To describe such phenomena, it is insufficient to use the systems of ordinary differential equations, which, in some cases, describe quite satisfactorily the complicated dynamic behavior of such integral characteristics as the reaction rate and the dimensionless coverage of the surface

with adsorbates. A very promising approach, being actively used in the recent decade for the description of interrelated and competing physicochemical processes on catalytic surfaces, is the imitation simulation of these processes by means of the statistical lattice models (Monte-Carlo technique). This approach makes it possible to describe most adequately the spatiotemporal dynamics of adsorbates on the catalytic surface.

Recently the statistical lattice model has been studied for the $(CO + O_2)/Pd(110)$ [6], which takes into account the change of surface properties due to the penetration of the adsorbed oxygen into subsurface layer. This model demonstrates oscillations in the rate of CO_2 formation and in the concentrations of the adsorbed species, as well as the autowave processes on the model palladium surface. But the model surface in our previous study [6] was assumed to be homogeneous, *i. e.*, the surface structure of the palladium single crystal was not taken into account. However it is well known, that CO or oxygen adsorption over the Pd(110) surface leads to the surface structure transformation [7] into the so called «missing row» structure: (1×1) → (1×2) (Fig. 1). The presence of steps introduces diffusion anisotropy and the diffusion rate of CO_{ads} along and across the rows can differ noticeably, *e. g.*, three times as many for the Pt(110) [8] (unfortunately, there is no experimental data for the Pd(110), for a review see [9]).

The anisotropy of surface diffusion should reflect in the shape of the chemical wave propagation observed in the oscillatory reaction regimes. In fact, elliptically shaped target patterns and spiral waves have been observed experimentally in numerous catalytic systems on stepped surfaces: CO oxidation on Pt(110) [10–12], H_2 oxidation on Rh(110) [13], NO + H_2 and H_2 + O_2 reactions on Rh(553) [14], *etc.* In our work we have studied the anisotropic effect of CO_{ads} diffusion on the reagent distribution over the surface and on the adsorbed species dynamics in the oscillatory regime of CO oxidation over Pd(110) using the statistical lattice model developed in [6] as a basis.

MODEL

The following reaction mechanism based on our FEM data was used in simulation [6]:

$$O_{2(gas)} + 2^* \rightarrow 2O_{ads} \quad (1)$$

$$CO_{gas} + {}^* \leftrightarrow CO_{ads} \quad (2)$$

$$CO_{ads} + O_{ads} \rightarrow CO_{2(gas)} + 2^* \quad (3)$$

$$O_{ads} + {}^*_v \rightarrow [{}^*O_{ss}] \quad (4)$$

$$CO_{ads} + [{}^*O_{ss}] \rightarrow CO_{2(gas)} + 2^* + {}^*_v \quad (5)$$

$$CO_{gas} + [{}^*O_{ss}] \leftrightarrow [CO_{ads}{}^*O_{ss}] \quad (6)$$

$$[CO_{ads}{}^*O_{ss}] \rightarrow CO_{2(gas)} + {}^* + {}^*_v \quad (7)$$

Here * and $^*_v$ are the active centres of the surface and subsurface Pd layer, respectively. Formation of the subsurface oxygen proceeds according to step 4, reduction of the initial surface – due to reactions (5) and (7) ("corkscrew" reaction). The adsorbed CO_{ads} species can diffuse over the surface according to the following rules:

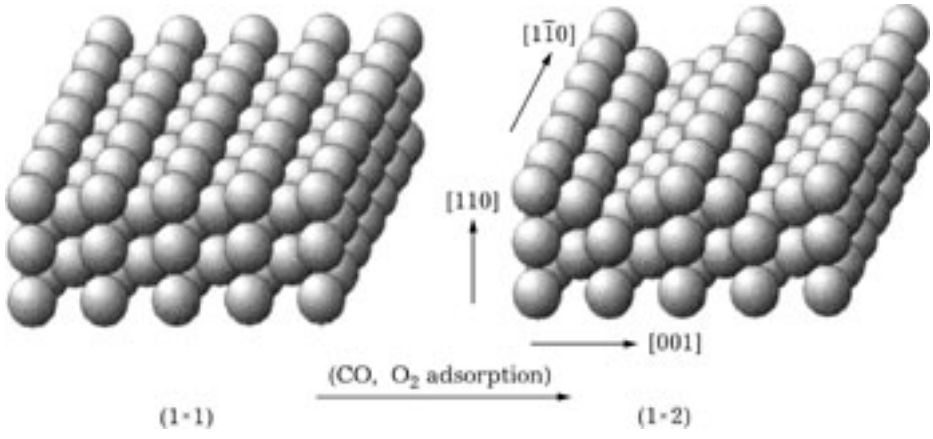

Fig. 1. Reconstruction of the Pd(110)–(1×1) surface into the (1×2) "missing-row" structure induced by adsorption.

i) $CO_{ads} + * \leftrightarrow * + CO_{ads}$

ii) $CO_{ads} + [*O_{ss}] \leftrightarrow * + [CO_{ads}{*}O_{ss}]$,

iii) $[CO_{ads}{*}O_{ss}] + [*O_{ss}] \leftrightarrow [*O_{ss}] + [CO_{ads}{*}O_{ss}]$

The simulation was performed on the lattice with a size of $N \times N$ square cells with periodic boundary conditions (for the most part of our simulations $N = 768$). Each lattice cell can exist in one of five states: *, CO_{ads}, O_{ads}, $[*O_{ss}]$, $[CO_{ads}{*}O_{ss}]$. The states of the cells are determined according to the rules specified by the detailed reaction mechanism. For steps 1, 2, −2, 4, 5, 6, −6, 7, the values of k_i were specified as a set of numbers, which can be considered as the rate coefficients of these elementary steps taking into account the partial pressures of O_2 (step 1) and CO (steps 2 and 6). That is, the values for O_2 and CO adsorption (k_1, k_2, and k_6) can be treated as a product of the impingement rate ($k_i \times P_i$) and of the sticking coefficient (S_i). The following set of the rate coefficients (s^{-1}) was used in simulation:

k_1	1
k_2	1
k_{-2}	0.2
k_4	0.03
k_5	0.01
k_6	1
k_{-6}	0.5
k_7	0.02

We suppose that reaction (3) proceeds immediately as soon as adsorbed CO_{ads} and O_{ads} appear in nearest neighbourhood. After each successful attempt of CO or O_2 adsorption as well as of CO_{ads} diffusion, the neighbouring cells were checked to find the partners in reaction (3). If the partners were found then the cells were given the state *, and one more CO_2 molecule was added to the reaction rate counter.

The method for processing the steps i)−iii) of CO_{ads} diffusion over the surface will be discussed below. The prescribed constants were recalculated as a probabilities of the realisation of elementary processes w_i by the formula: $w_i = k_i / \Sigma k_i$. Using a generator of random numbers uniformly distributed over the (0, 1) interval, we chose one of these processes according to the specified ratio of their occurrence (the "comb" of probabilities). Then, also using pairs of random numbers, the coordinates of one cell (or two adjacent cells, depending on the chosen process) were determined from $N \times N$ cells of lattice. This algorithm (first, choice of the process and second, choice of the cell) makes it possible to take into account the dependence of the step rates on the adsorbate coverage. The detailed description of the algorithm can be found in [6].

The so-called MC-step (MCS) consisting of $N \times N$ attempts of choice and realisation of "main" elementary processes (1)−(2), (4)−(7) is used as a time unit in the Monte-Carlo models. During the MCS, each cell is tested on the average once. The reaction rate and surface coverages were calculated after each MCS as a number of CO_2 molecules formed (or the number of cells in the corresponding state) divided by the total value of the lattice cells N^2. In the course of each MCS after every choice of one of the above-named processes and an attempt to perform this process the inner cycle of CO_{ads} diffusion was processed, which included ($M_x + M_y$) attempts of random choice of a pair of adjacent cells of the lattice. For the sake of simplicity we did not model in direct way the process of (1×1) → (1×2) surface reconstruction, we only proposed that the intensity of CO_{ads} diffusion was different in x (M_x attempts) and in y (M_y attempts) directions on our square lattice representing the catalytic surface (diffusion anisotropy, x is the $[1\bar{1}0]$ direction). If the $\{CO_{ads}, *\}$, $\{CO_{ads}, [*O_{ss}]\}$, $\{*, [CO_{ads}{*}O_{ss}]\}$, $\{[CO_{ads}{*}O_{ss}], [*O_{ss}]\}$ pairs turned out to be the chosen pairs, the states in these cells were interchanged according to the rules i)−iii), *i. e.* diffusion took place. Otherwise, the attempt of diffusion was rejected.

RESULTS AND DISCUSSION

Parameters of the model: diffusion intensity of CO_{ads} molecules

Calculations of the diffusion intensity were performed in suggesting that this process can be described with usual Arrhenius relationship [15]: $D = D_0 \exp\{-E_m / k_B T\}$. Here E_m, the activation energy of surface migration, is from

1/3 to 1/10 of activation energy of desorption, and the pre-exponential factor D_o is from 10^{-2} to 10^{-4} cm^2/s. For CO on the Pd(110) plane E_m = 6–10 kcal/mol. It is known [16], that for Pd(111) plane E_m = 9.5–12 kcal/mol, D_o = $10^{0\pm2}$ cm^2/s. Therefore we used in calculations the values E_m = 10 kcal/mol и D_o = 10^{-2} cm^2/s. At 400 K it gives diffusion mobility of the CO molecule $(<X^2>)^{1/2}$ = 2.7 10^{-4} cm per one second or ~10^4 of active sites, taking into account that the size of a palladium atom r = 2.75 Å. If 1s = 10^3 MCS, during 10^{-3}s (1 MCS) every molecule of CO diffuse along the surface at average as far as 10 cells. Assuming, that for every attempt of diffusion one molecule of CO visits one cell, for the entire surface (in the particular case for N = 100) it gives $10\times100^2 = 10^5$ attempts of diffusion for 1 MCS as a minimum. This value is in very good agreement with the number of attempts, used in our simulations ($N\times N\times M$ = 100×100×100 = 10^6 of attempts, as a rule).

Parameters of the model: rate coefficients of elementary steps

Experimental values of the rate coefficients for elementary steps of the reaction as well as a set of values k_i at which one can obtain the oscillatory regime both of the rate of CO_2 formation and of the surface coverages (see below) are presented in Table 1. The values of k_i at the pressure 10^{-2} Torr are presented as well, relatively of the rate of CO adsorption, as of the best consisted with parameters, used in modeling. The only exception is the rate of oxygen adsorption. It can be explained by the following. It is well known that the sticking coefficient of oxygen decreases with increasing of the surface coverage [4, 17, 18], moreover, the presence of the subsurface oxygen layer reduces this coefficient by two orders of magnitude [19]. Hence, it would result in decrease of the relative rate of adsorption $k_{\mathrm{adsO}}/k_{\mathrm{adsCO}}$ (exp). It can be seen from the Table 1, that the rates of the steps 4, 5 and 7 are low, in comparison with others, and the rate of reaction CO_{ads} + O_{ads} is much higher than the rates of others steps, as has been supposed during the simulations. One can agree that the prescribed values

TABLE 1

Elementary step of reaction	Rate constants	E_i, kcal/mol	ν_i, 1/s	k_i (exp), T = 400 K	References	k_i (exp)/k_{adsCO} (exp), $P = 10^{-2}$ Torr	k_i (model)
Adsorption of O_2	k_1	0		7.6 10^5 1/(s Torr)	[17]	2 · (10^2–10^3)	1
Adsorption of CO	k_2	0		4.1 10^5 1/(s Torr)	[4]	1	1
Desorption of CO	k_{-2}	24	4.35 10^{13}	3.0 1/s	[4]	1 · (10^{-1}–1)	0.2
Reaction O_{ads} + CO_{ads}	k_3	14	8.6 10^9	1.8 10^2 1/s	[4]	5 · (1–10)	∞
Diffusion $O_{ads} \rightarrow O_{ss}$	k_4	10	3.0 10^4	9.8 10^{-2} 1/s	[4]	3 · (10^{-3}–10^{-2})	0.03
Diffusion $O_{ss} \rightarrow O_{ads}$	k_{-4}	28	2.5 10^{12}	1.1 10^{-3} 1/s	[4]	4 · (10^{-5}–10^{-4})	0
Reaction O_{ss} + CO_{ads}	k_5						0.01
Diffusion of CO	*i*)–*iii*)	10	10^{-2} cm^2/s	3.6 10^{-8} cm^2/s		>10^5 attempts	10^6
Formation of [CO_{ads} O_{ss}]: CO_{gas} + [*O_{ss}] → [CO_{ads} O_{ss}]	k_6						1
Decomposition of [CO_{ads} O_{ss}]: [CO_{ads} O_{ss}] → CO_{gas} + [*O_{ss}]	k_{-6}						0.5
Reaction in [CO_{ads} O_{ss}] : [CO_{ads} O_{ss}] → CO_2 + * + *v (“corkscrew reaction”)	k_7						0.02

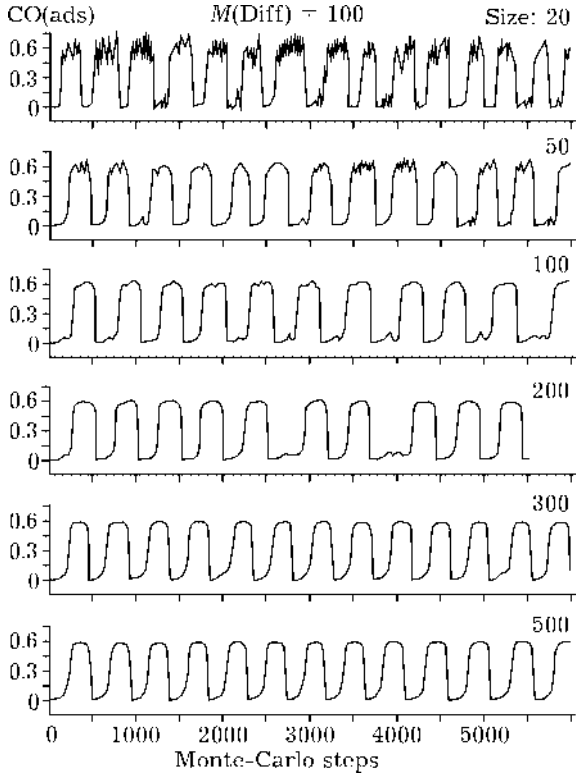

Fig. 2. Dynamics of CO_{ads} at different lattice size values N (for the values of other parameters see text).

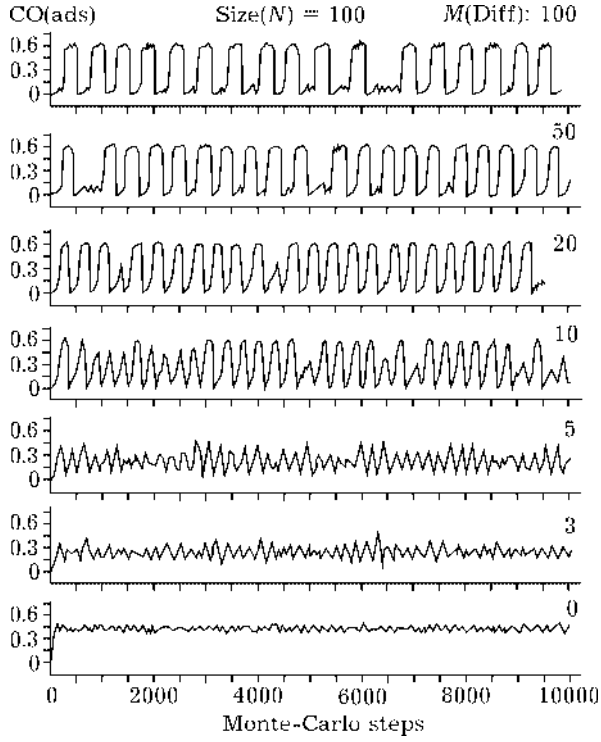

Fig 3. Dynamics of CO_{ads} at different diffusion intensities (isotropic diffusion) M (for the values of other parameters see text).

of elementary steps are in good agreement with experimental data.

Variation of the lattice size N

The effect of stabilization of period of oscillation was observed during increasing of the lattice size from 300×300 to 500×500 cells (Fig. 2). Amplitude and period of oscillations does not change. During decreasing of the lattice size the oscillations become less regular. The fluctuations of the surface coverages increase markedly during the period of oscillations but the oscillatory regime do not vanish. It is obvious that with further decreasing of the lattice size the fluctuation component will only increase due to decreasing of the amount of sampling.

Variation of the diffusion intensity M

The influence of the CO_{ads} diffusion intensity on the character of oscillations was investigated as well. It was shown (see Fig. 2 in ref. [6]) that by the increase of the diffusion intensity $M = M_x + M_y$ ($M_x = M_y$ – isotropic diffusion) more than 50 (at sufficiently large lattice size $N = 500$), oscillations do not change practically. Decreasing of the diffusion rate (Fig. 3) results in dividing of the surface into several regions, which are weakly bound with each other, and oscillate with the same period, but with a little shift in phase. This means that the role of diffusion consist in the synchronization of the oscillations over the surface.

Anisotropic effect

The simulation of oscillations with anisotropic diffusion was performed on the lattices with N varied from 500 to 1500 cells at the ratio of the diffusion cycle parameters M_x/M_y being equal to 75/25, 80/20 and 85/15. The values of the rate coefficients are referred above. Surprisingly, but the integral oscillations of the reaction rate and of the surface coverages (Fig. 4) do not vary with the change of the ratio M_x/M_y and do not differ from the case with isotropic diffusion $M_x = M_y = 50$ [6]. The amplitude, the period and the shape of oscillations remain invariable.

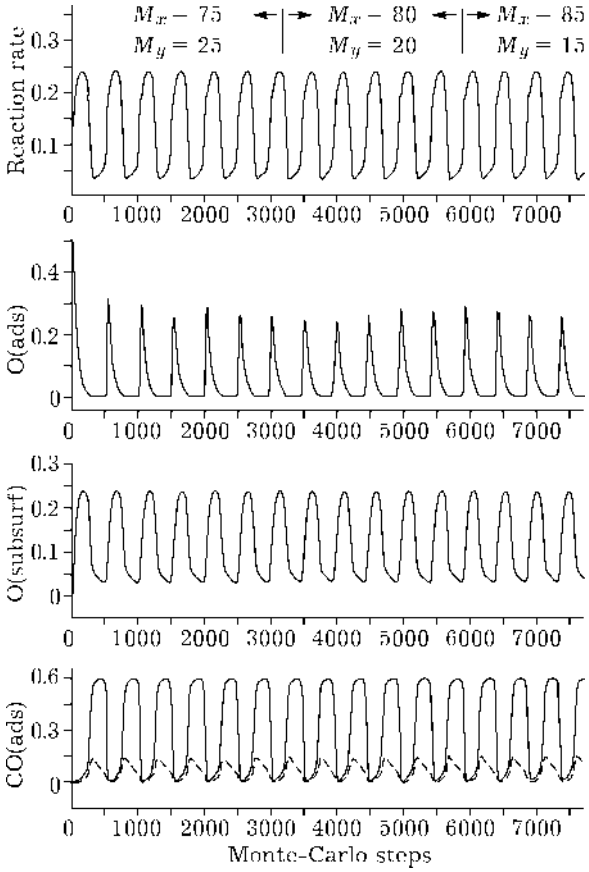

Fig. 4. Dynamics of changes in surface coverages CO(ads) = CO_{ads} (solid line) and [CO_{ads}*O_{ss}] (dash-dotted line), O(subsurf) = *O_{ss}, O(ads) = O_{ads} and the specific reaction rate at different ratios M_x/M_y (the instants of switching of diffusion parameters are shown by arrows). N = 768, the rate coefficients are listed in the Table 1.

But the chemical wave pattern observed on the model surface in the oscillation regime becomes anisotropic and the shape of the propagation of the reaction fronts reflects the increasing value of the M_x/M_y ratio. This signifies that the kinetic measurements of the reaction rate and concentrations only could not reveal the anisotropic effect of the adsorbed species diffusion, this effect could be observed only by using the physical methods for the direct surface imaging. Let us compare the simulated snapshots showing the adsorbate distribution over the surface during surface oxygen wave propagation at the instants of the reaction rate ignition (see Fig. 4). For the correct comparison the snapshots are chosen having the approximate equal oxygen coverages (O_{ads} ~ 0.05) and different M_x/M_y (Fig. 5). The snapshots show the elliptically deformed along the [1$\bar{1}$0] direction (in our case x direction) oxygen islands surrounded by the narrow regions with elevated concentration of the free active centers, the so-called reaction zone [6]. Due to the rapid O_2 adsorption and subsequent fast reaction with neighboring CO_{ads} the formation of CO_2 molecules proceeds most intensively just in that reaction zone. The existence of the "reaction zone" was found experimentally (field ion probe-hole microscopy technique with 5 Å resolution) in [20].

More obviously the dynamics of the anisotropic effect could be seen in observation of the steadily existing spatio-temporal structures on the surface, *e. g.*, the spiral waves. Fig. 6 illustrate the evolution of the simulated spiral wave in CO oxidation reaction over Pd(110) after the switching the diffusion intensity from isotropic regime (M_x/M_y = 50/50) to the anisotropic one (M_x/M_y = 80/20). The manner to come into the spiral wave regime of the oscillation is described in [21]. Fig. 6, *a* show the

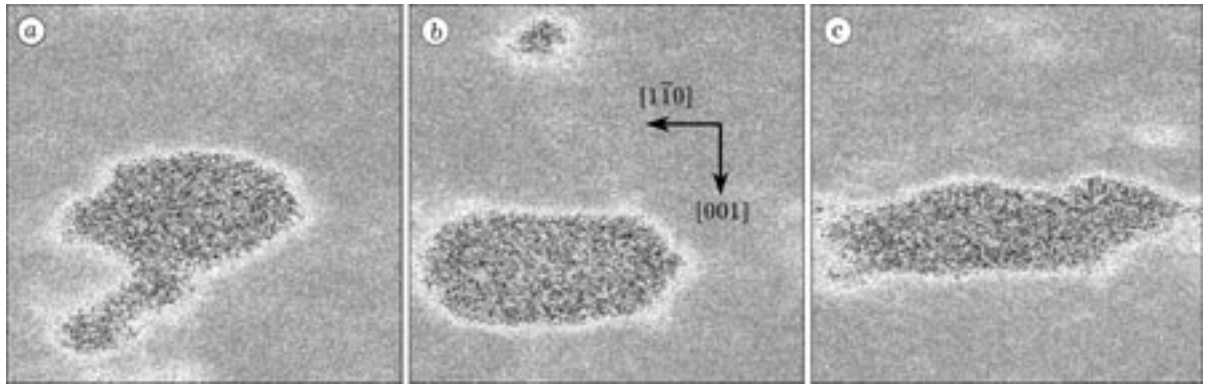

Fig. 5. Snapshots reflecting the adsorbate distribution over the surface during oxygen wave propagation: O_{ads} is black, O_{ss} is 75 % grey, CO_{ads} is 50 % grey, [CO_{ads}*O_{ss}] is 25 % grey and the adsorbate-free surface is white: *a* – 2979 MCS, M_x/M_y = 75/25; *b* – 3951 MCS, M_x/M_y = 80/20; *c* – 7344 MCS, M_x/M_y = 85/15.

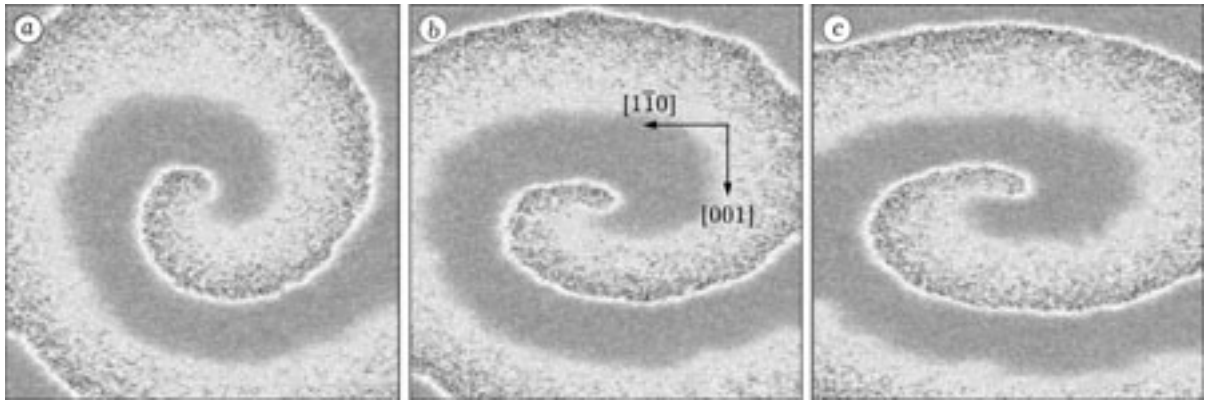

Fig. 6. Evolution of the simulated spiral wave in CO oxidation reaction over Pd(110) after the switching at MCS = 10 000 the diffusion intensity M from isotropic regime (M_x/M_y = 50/50) to the anisotropic one (M_x/M_y = 80/20): a – 10 010 MCS; b – after first spiral rotation – 10 350 MCS; c – after second spiral rotation – 10 700 MCS.

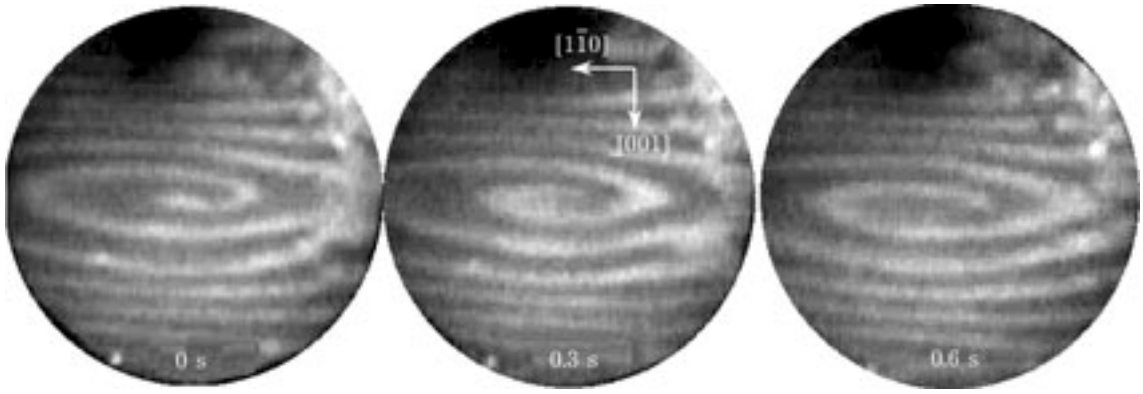

Fig. 7. PEEM images of the surface spiral waves in CO oxidation reaction over Pd(110) [22]: $P(O_2)$ = 4 10^{-3} Torr, P(CO) = 1.6 10^{-5} Torr, T = 349 K. Dark regions – CO_{ads}, bright regions – O_{ads} – corresponds to the different work function values.

shape of the spiral wave right away after the switching the diffusion intensity (at 10 000 MCS), Figs. 6, *b* and 6, *c* demonstrates the stretching of the spiral wave after the first and second rotation correspondingly. Let us compare the simulated anisotropic effect with the experimental observation of the spiral waves in CO oxidation reaction over Pd(110) single crystal obtained by means of Photoemission Electron Microscopy (PEEM) in [22]. It has been obviously seen in the Fig. 7 that the spiral wave displays an anisotropy according to the crystal symmetry in [1$\bar{1}$0] direction.

CONCLUSION

It has been established that the adsorbed CO diffusion anisotropy, which is the result of the surface phase transition (1×1) → (1×2) induced by reagents adsorption (not modeled in direct way in our study), does not influence the oscillation kinetics but leads to the appearance of the propagating reaction fronts on the palladium surface elliptically stretched along the [1$\bar{1}$0] direction in close agreement with the known experimental data.

Acknowledgement

The financial support of the INTAS Grant No. 99–01882, RFBR Grant No. 02–03–32568 and Zamaraev International Charitable Scientific Foundation is highly appreciated.

REFERENCES

1 M. Ehsasi, C. Seidel, H. Ruppender *et al.*, *Surf. Sci.*, 210 (1989) L198.
2 S. Ladas, R. Imbihl and G. Ertl, *Ibid.*, 219 (1989) 88.
3 B. C. Sales, J. E. Turner and M. B. Maple, *Ibid.*, 114 (1982) 381.

4 M. R. Basset and R. Imbihl, *J. Chem. Phys.*, 93 (1990) 811.
5 A. L. Vishnevskii, V. I. Elokhin and M. L. Kutsovskaya, *React. Kinet. Catal. Lett.*, 51 (1993) 211.
6 E. I. Latkin, V. I. Elokhin, A. V. Matveev and V. V. Gorodetskii, *J. Mol. Catal. A: Chem.*, 158 (2000) 161.
7 H. Tanaka, J. Yoshinobu and M. Kawai, *Surf. Sci.*, 327 (1995) L505.
8 H. H. Rotermund, S. Nettesheim, A. von Oertzen and G. Ertl, *Ibid.*, 275 (1992) L645.
9 M. U. Kislyuk, *Kinetika i kataliz*, 39 (1998) 246 [*Kinet. Catal.*, 39 (1998) 229, Engl. Transl.].
10 A. von Oertzen, H. H. Rotermund and S. Nettesheim, *Surf. Sci.*, 311 (1994) 332.
11 S. Jakubith, H. H. Rotermund, W. Engel *et al., Phys. Rev. Lett.*, 65 (1990) 3013.
12 A. J. Patchett, F. Meißen, W. Engel *et al.*, *Surf. Sci.*, 454–456 (2000) 341.
13 F. Mertens and R. Imbihl, *Chem. Phys. Lett.*, 242 (1995) 221.
14 A. Schaak, B. Nieuwenhuys and R. Imbihl, *Surf. Sci.*, 441 (1999) 33.
15 O. V. Krylov and B. R. Shub, Non-equilibrium Processes in Catalysis, Khimiya, Moscow, 1999 (in Russian).
16 R. Imbihl, *Progr. Surf. Sci.*, 44 (1990) 185.
17 J. Goschnick, M. Wolf, M. Grunze *et al.*, *Surf. Sci.*, 178 (1986) 831.
18 K. Yagi, D. Sekibo and H. Fukutani, *Ibid.*, 442 (1999) 307.
19 M. P. Kiskinova, Poisoning and Promotion in Catalysis Based on the Surface Concepts and Experiments, Elsevier, Amsterdam, 1992.
20 V. V. Gorodetskii and W. Drachsel, *Appl. Catal. A: General,* 188 (1999) 267.
21 E. I. Latkin, V. I. Elokhin and V. V. Gorodetskii, *Chem. Eng. J.*, 91 (2003) 123.
22 J. H. Block, M. Ehsasi, V. Gorodetskii *et al.*, in T. Inui *et al.* (Eds.), New Aspects of Spillover Effect in Catalysis, Stud. Surface Sci. & Catal., vol. 77, Elsevier Sci. Publ. B.V., 1993, pp. 189–194.